Development and Optimisation of Textile-Based Optical Sensors for Cardiac Health Monitoring

Tharushi Peiris
Nottingham School of Art and Design
Nottingham Trent University
Nottingham, United Kingdom
0009-0009-6122-8897

Arash Shahidi
Nottingham School of Art and Design
Nottingham Trent University
Nottingham, United Kingdom
0000-0002-7780-3122

Demosthenes Koutsogeorgis
School of Science and Technology
Nottingham Trent University
Nottingham, United Kingdom
0000-0001-6167-1084

William Hurley
Nottingham School of Art and Design
Nottingham Trent University
Nottingham, United Kingdom
0000-0003-0521-7156

Carlos Oliveira
Nottingham School of Art and Design
Nottingham Trent University
Nottingham, United Kingdom
0000-0001-8143-3534

Tilak Dias
Nottingham School of Art and Design
Nottingham Trent University
Nottingham, United Kingdom
0000-0002-3533-0398

Theo Hughes Riley
Nottingham School of Art and Design
Nottingham Trent University
Nottingham, United Kingdom
0000-0001-8020-430X

***Abstract*—Wearable cardiac health monitoring could play a crucial role in managing an individual's cardiac health conditions. This study focuses on the development and optimisation of a textile-based optical sensor system utilising photoplethysmography (PPG) technology for continuous cardiac health monitoring. Light Emitting Diode (LED) and Photodiode (PD) electronic yarns were engineered by embedding these components into textile yarns. This is achieved by first soldering the component onto Litz wires, then by encapsulating the component inside a protective resin pod, and finally by covering the component in a braided structure. The optical properties of the E-yarns were optimised by exploring various resin micro-pod configurations and braiding techniques. The optical behaviours (transmission and reflectance as a function of wavelength) of the resin pods have been characterised. A prototype, knitted textile glove capable of monitoring blood volume variations and generating PPG waveforms has been realised. This system was validated by recording pulse rate (PR) readings from ten human subjects confirming its functionality and accuracy as a textile-based optical sensing system. This work demonstrates significant progress in integrating advanced optical sensors into wearable textile platforms, promising enhanced functionality for cardiac health monitoring applications.**

Keywords—Wearable health monitoring, Optical sensor, Photoplethysmography (PPG), Electronic yarn, Electronic textile

I. Introduction

In the healthcare and wellness domain, wearable technologies have become integral, enabling unobtrusive, non-invasive, and continuous long-term monitoring of physiological parameters. These wearable systems enable advanced and precise medical diagnostics facilitating early detection and prevention [1], [2], [3], [4]. Among the various sensing mechanisms employed in wearables, electro-optical sensors play an instrumental role in detecting electromagnetic radiation across a range of diverse wavelengths and converting them into electronic signals. Traditional cardiovascular health monitoring has been fundamentally transformed towards non-invasive and continuous approaches, with the integration of optical sensors into wearables [5].

Given the paramount importance of cardiac health surveillance, especially as cardiovascular diseases account for one-third of global deaths [6], these advancements offer vital capabilities. Despite electrocardiography (ECG) being the clinical standard for cardiac monitoring, its limitations in sporadic monitoring do not capture infrequent cardiac events and trends which reflect subtle changes, while wearables with continuous monitoring enable early intervention and personalised management of physiological conditions [3], [7].

Photoplethysmography (PPG) technology uses light sources and optical sensors to measure blood volume variations and has become a widely adopted non-invasive mechanism for optically monitoring cardiac health. With its precision and accuracy, PPG emerges as a prominent solution following ECG for monitoring heart activity. PPG operates on the principle of illuminating light towards subcutaneous tissue and detecting variations in the light intensity, providing information on pulse rate (PR) [8], pulse rate variability (PRV) [9], blood oxygen saturation [10] and blood pressure [11]. PPG technology is identified as a reliable alternative for ECG, with a correlation recognised between heart rate and heart rate variability measurements obtained through ECG and the corresponding PR and PRV recorded by PPG sensors [12], [13].

PPG data acquisition employs either transmission mode, where light passes through tissue, or reflection mode, with both light source and the detector positioned adjacent to the skin [13]. PPG sensors can be designed with either single or multiple wavelengths, depending on the specific cardiac parameters being monitored with the system. A variety of wearable PPG sensors for cardiac health measurement has been developed with optical fibres [14], printed electronics [15], organic [16], and inorganic [17] optical components.

Traditional methods of assembling optical sensors often rely on bulky and rigid electronics [10]. In contrast, textiles provide a more comfortable and seamless integration of electronic components.

This paper presents the development and optimisation of PPG-based optical sensors integrated into textile yarns for

cardiac health monitoring. The goal is to embed light-emitting diodes and photodiodes into textile yarns and create a PPG system, providing a comfortable and flexible solution for real-time cardiac health assessment. The integration of optical components into textiles poses challenges related to optical behaviour and sensor performance, which are addressed through the optimisation of the process parameters and materials. Further, a prototype knitted glove integrated with the optical sensing E-yarns capable of recording PPG signals in transmission mode has been developed and its accuracy has been validated through human trials.

II. Materials and Methods

A. Resin Micro-pod Optical Characterisation

The encapsulation process for the optical components needed to be optimised to maximise the accuracy of the final sensor system. The encapsulation process involves various parameters such as resin type, resin pod shape, surface smoothness, width, and thickness, which all affect the optical performance of the embedded component. These parameters influence light behaviour through factors such as absorption, scattering, and reflection. For optimal component positioning and to minimise light scattering, smooth, flat-surfaced, rectangular resin micro-pods were selected for use throughout the E-yarn fabrication and characterisation process.

Optical transmittance and reflectance of several micro-pod types were explored. The optical characterisation focused initially on two resin types, R1 and R2 with five thickness variations ranging from 1.5 mm to 2.5 mm, and two width variations of 1.5 mm and 2.0 mm, with one sample of each design investigated. The transmittance and reflectance of these resin micro-pods were measured across a wide, relevant, wavelength range from visible light (400 nm) to near-infrared (NIR) (2500 nm) using OceanOptics NIR256 spectrometer (Orlando, FL, USA) and OceanOptics USB4000 spectrometer (Orlando, FL, USA) with SpectraSuite software as illustrated in Fig. 1(a). Statistical tests including analysis of variance and regression analysis were performed to determine the significance of each variable's impacts towards the optical properties and to quantify the relationships. To confirm the consistency of the observed optical behaviours, further testing was conducted with three resins: R1, R2 and R3 using repeatable samples (n = 5) for a selected resin pod width and thickness (w = 2 mm, t = 2.5 mm) as shown in Table 1.

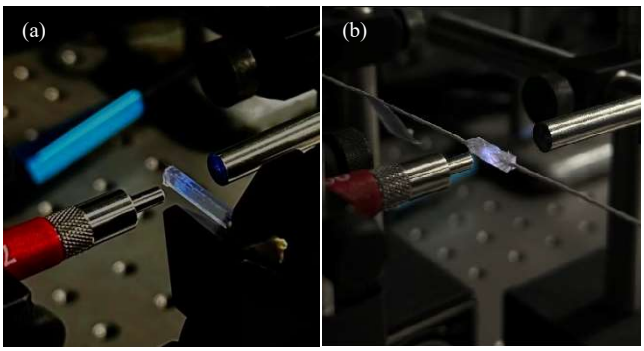

Fig. 1. Photograph of the experimental set-up showing the optical characterisation of resin micro-pods and resin micro-pods within a braided structure. (**a**) Transmittance of encapsulation. (**b**) Transmittance of a resin micro-pod within a braided structure.

TABLE I. Details of Resins Explored

Resin	Company	Composition	Water Absorption (25^0C 24h)
R1 - 9001 E-V3.5	Dymax Corporation (Torrington, USA)	Acrylated Urethane	1.0%
R2 - 9001-E-V3.7	Dymax Corporation (Torrington, USA)	Modified Urethane	1.0%
R3 - Light weld 429	Dymax Corporation (Torrington, USA)	Acrylated Urethane	1.1%

B. Braid Structure Optical Characterisation and Optimisation

Following the encapsulation characterisation, a preliminary evaluation of the braiding process was conducted with a fixed micro-pod size (w = 1.5 mm, t = 1.5 mm, l = 12 mm) and resin material (resin R1, selected following the encapsulation optical study), to analyse the impact of the number of covering yarns and lay length. The initial analysis focused on two yarn carrier configurations of the braided yarn: B1 - 12 yarn carriers and B2 - 24 yarn carriers with lay lengths of: L1 - 5 mm, L2 - 10 mm, L3 - 15 mm. The experimental setup is illustrated in Fig. 1(b).

The braid was constructed using a textile braiding machine (Herzog RU 1/24-80; Oldenburg, Germany) using white polyester yarns (1 ply, 167 Dtex, 48 filaments; J. H. Ashworth & Son Ltd, Hyde, UK). Polyester was selected as the covering yarn due to its superior coverage and reduced hairiness, which enhances the smoothness of the final braided structure, making it more suitable for embedding optical components in wearable textile applications.

C. Prototype Pulse Rate Monitoring Glove Construction

The fabrication of the optical sensing E-yarns needed for the glove prototype began with the critical selection of optical components and circuit designing. LEDs are most commonly used as the light source and PDs are preferred as sensors for their high sensitivity and quick response times. Among the various types of PDs, literature suggests PIN photodiodes as highly effective in developing PPG sensors. In this study, a LED (IN-S42CTQHIR; Inolux, Santa Clara, CA, USA) with a peak wavelength (940 nm) in the NIR range was selected to align with the peak sensitivity (820 nm) of the selected PIN PD (VEMD6060X01; Vishay Intertechnology, Malvern, PA, USA) (the same component as explored in [18]) to be embedded within textiles to create optical sensing E-yarns.

Separate E-yarns were produced for both the LED embedded E-yarn and the PD embedded E-yarn to emit and detect light respectively. In both cases the fabrication process involved soldering the selected component onto two Litz wires (outer diameter = 254 µm; BXL2001, OSCO Ltd., Milton Keynes, UK).

The soldered components were then paired with a high-strength multifilament yarn (VECTRAN™, Kuraray America, Inc., Houston, TX, USA) and encapsulated within a micro-resin pod with the optimised pod dimensions and using the selected resin based on the optical characterisation experiments, to create a robust yarn. The encapsulated components and wires were then covered with the selected textile yarns and braided with a braid created using the optimised braiding parameters identified from the braid structure characterisation. The process steps of these E-yarn manufacturing are illustrated with Fig. 2.

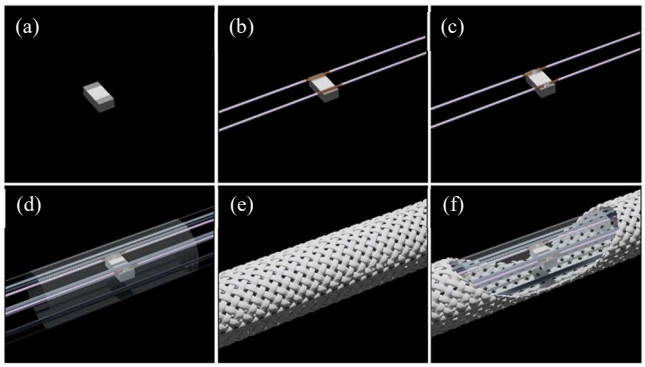

Fig. 2. Graphical illustration of the E-yarn manufacturing process. (**a**) Optical component. (**b**) Optical component placed on Litz wires. (**c**) Optical component soldered onto Litz wires. (**d**) Optical component encapsulated within the resin micro-pod along with supportive yarns. (**e**) Braided E-yarn. (**f**) E-yarn structure with cut-away showing interior details.

The prototype glove was created using a 3D seamless flat knitting machine (Stoll ADF32W, 7.2 gauge; Karl Mayer Stoll GmbH, Obertshausen, Germany) with a single jersey base structure, a rib structured cuff area and two tubular channels. It was composed of white fluid yarns (1 ply, 2 % elastane, 7 % nylon, 91 % viscose; Yeoman Yarns Ltd, Leicester, UK), combed cotton yarns (1 ply, 24 count; YEOMAN yarns Ltd, Leicester, UK), and nylon 6/6 yarns (2 ply, 78 Dtex, 68 filaments; Contifibre S.p.A., Casaloldo, Italy). The PD E-yarn and LED E-yarn were integrated into the two knitted channels on the inner side and outer side of the index finger, respectively.

D. Validation of the Prototype Pulse Rate Monitoring Glove

The prototype pulse rate monitoring glove was validated by recording signal outputs of ten human subjects wearing the prototype on the right hand, while in rest. The participants consisted of an equal distribution of males and females, ranging from age 18 to 36 years. Ethical approval was obtained to conduct these human trials from the Nottingham Trent University Schools of Art and Design, Architecture, Design, and Humanities Research Ethics Committee (Application ID 1843617, date of approval 22nd July 2024). Informed consent was obtained from all participants before the study and the recorded data is stored in a data archive.

Measurements from the prototype glove were taken by powering the LED yarn integrated within the glove with an Arduino Mega (2560), which provided a 2.5 V output and recording the output signal of the integrated PD yarn in reverse bias through the Keithly DAQ6510 Data Acquisition and Logging Multimeter system (Tektronix UK Ltd, Oldbury, UK): The signal was recorded using a Keithley 7710 Solid-state Differential Multiplexer. Five sequential signal readings of each person were recorded for a one minute duration with 40 ms data intervals (minimum data scan interval of the DAQ system).

Concurrently, five pulse rate readings were recorded at the same time, using Masimo Rad-67 CO-Oximeter (Masimo Corporation, CA, USA) connected to the index finger of the left hand of the participant, to compare against the processed readings recorded from the developed system and validate its functionality.

III. Results

A. Encapsulation Characterisation Results

The optical test results when using resin R1 and R2, with varying resin pod thicknesses and widths, were analysed to distinguish their transmittance and reflectance behaviours. Fig. 3 shows the transmission behaviour of the two resins across varying thicknesses. Due to the limited number of width variations, its impact is discussed with statistical analysis rather than a graphical representation.

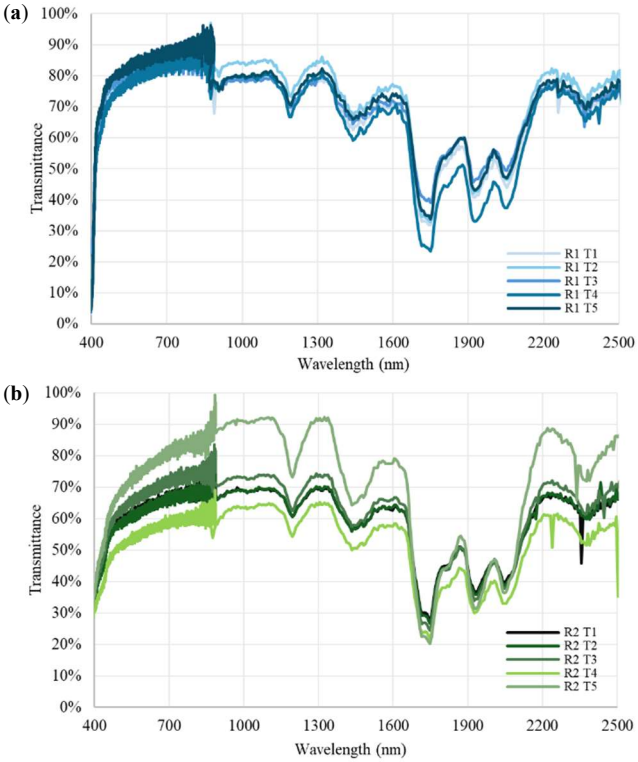

Fig. 3. Characteristic transmission behaviour of two different resin micro-pod types for five thicknesses of micro-pod. (**a**) 9001-E-V3.5 (R1). (**b**) 9001-E-V3.7 (R2)

The transmittance analysis demonstrated that resin type has a significant impact on light transmission, with R1 showing a higher transmission of over 80 % across all thicknesses in the visible light range, while R2 showed lower transmission levels (over 50 %), as illustrated in Fig 3. Analysis of variance (ANOVA) tests were conducted to identify the significance of the resin type towards transmission behaviour and confirmed that the resin type has a statistically significant impact ($p < 0.05$), whereas the ANOVA to identify the impact of thickness and width on transmission confirmed no major influence ($p > 0.05$) over the visible and NIR wavelength ranges as shown in Table 2.

TABLE II. Analysis of Variance Test Results on Transmittance Behaviour

	P Value	
	Visible wavelength range	**NIR wavelength range**
C(Resin)	0.00329	0.017960
C(Thickness)	0.174064	0.282483
C(Thickness)	0.339450	0.327357
C(Width)	0.195711	0.147584

The reflectance readings showed that both resins reflected less light across the wavelengths of interest, with reflection under 10 %, where R2 reflected comparatively less light than R1, as illustrated in Fig 4. ANOVA tests performed to quantify the significance of the impact of resin type denoted that the variation in reflectance between the resin types has no statistical influence. The p-values obtained with the ANOVA tests, as shown in Table 3, confirm the statistical significance of each factor's impact on reflectance variations. Moreover, neither width nor thickness had a significant influence on the reflectance behaviour.

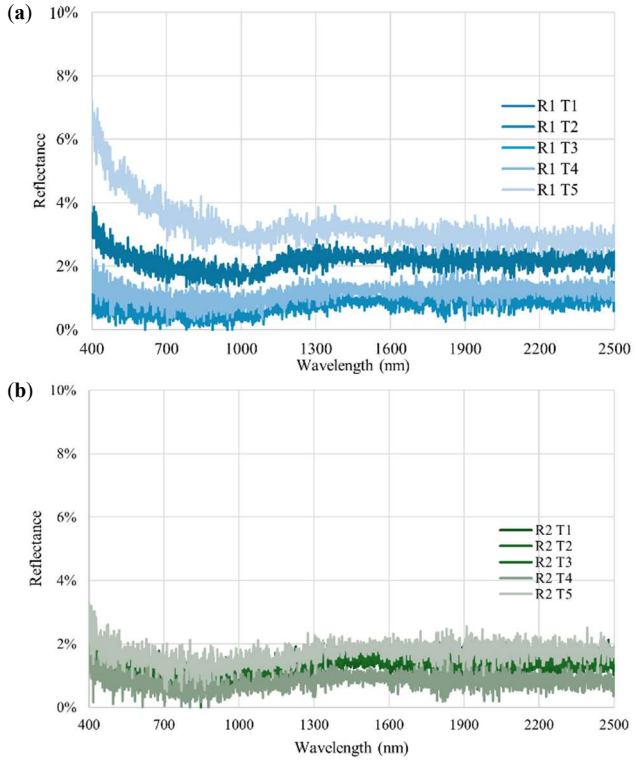

Fig. 4. Characteristic reflectance behaviour of two different resin micro-pod types for five thicknesses of micro-pod. (**a**) 9001-E-V3.5 (R1). (**b**) 9001-E-V3.7 (R2).

TABLE III. ANALYSIS OF VARIANCE TEST RESULTS ON REFLECTANCE BEHAVIOUR

	P Value	
	Visible wavelength range	**NIR wavelength range**
C(Resin)	0.140437	0.078132
C(Thickness)	0.950557	0.751715
C(Width)	0.927171	0.968854

Optical characterisation was then conducted using three resins with one micro-pod size, the resulted transmittance and reflection behaviours are graphically represented with Fig. 5.

Resin R1 showed the highest transmission over the other two resins which was confirmed with the coefficient values gained through the regression analysis results, given in Table 4. Resin R3 displayed a transmittance level slightly lower than R1, while R2 showed significantly lower transmittance. In terms of reflectance, all three resins showed less reflectance under 10 %, where R2 showed the lowest followed by R1 and R3.

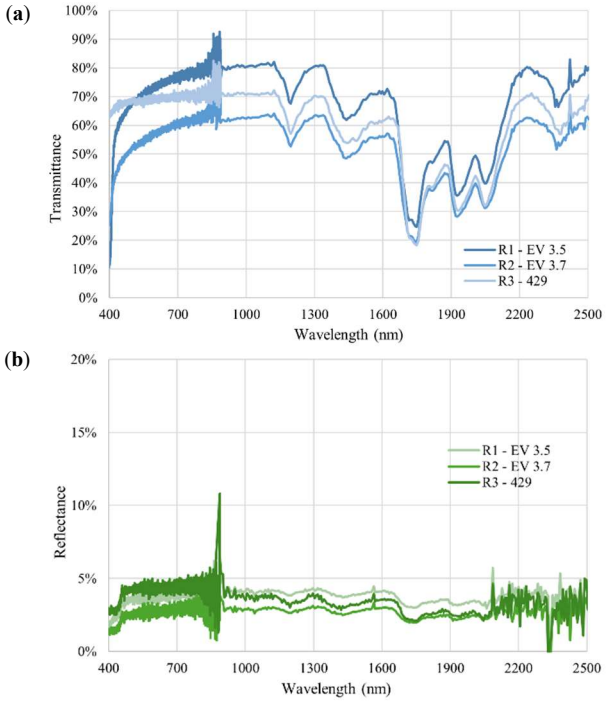

Fig. 5. Characteristic optical behaviour of micro-pods made with three different types of resin. Each dataset is the average of five repeat samples. (**a**) Transmittance behaviour. (**b**) Reflectance behaviour.

TABLE IV. REGRESSION ANALYSIS FOR THE TRANSMITTANCE AND REFLECTANCE BEHAVIOUR OF THREE RESIN TYPES

		Visible Wavelength Range		NIR Wavelength Range	
		Coefficient	**P-value**	**Coefficient**	**P-value**
Transmittance	Intercept (R1)	0.6617	0.000	0.7671	0.000
	C (Resin: R2)	-0.1354	0.004	-0.1526	0.005
	C (Resin: R3)	0.0201	0.609	-0.0880	0.072
Reflectance	Intercept (R1)	0.0348	0.000	0.0392	0.000
	C (Resin: R2)	-0.0098	0.147	-0.0107	0.139
	C (Resin: R3)	0.0059	0.373	0.0003	0.969

Different levels of consistency were identified within the resin types with the standard deviation values presented in Table 5, where R1 and R3 showed much reliability compared to R2 across both visible and NIR wavelength ranges.

TABLE V. STANDARD DEVIATION OF RESULTS AMONGST RESIN SAMPLES

	Resin	**Visible Wavelength Range**	**NIR Wavelength Range**
Transmittance	R1	0.046579	0.058108
	R2	0.083883	0.099788
	R3	0.041529	0.039710
Reflectance	R1	0.009478	0.010204
	R2	0.008326	0.010168
	R3	0.011881	0.011731

The objective of this optical characterisation was to identify the factors influencing the transmittance and

reflectance characteristics of the encapsulated resin micro-pods and to optimise these optical behaviours to have high transmittance and lower reflectance. Hence, resin R1 (Dymax 9001 E-V3.5) was selected due to its high light transmittance behaviour and moderately low reflectance, to be used in further experiments. As the width and thickness of the resin micro-pod were identified to have no significant influence on the optical behaviour, micro-pod dimensions were defined based on the component size, with an intention to minimise the size of the micro-pod as much as possible.

B. Braiding Characterisation Results

The optical characterisation of micro-pods covered in a braided structure are presented in Fig. 6.

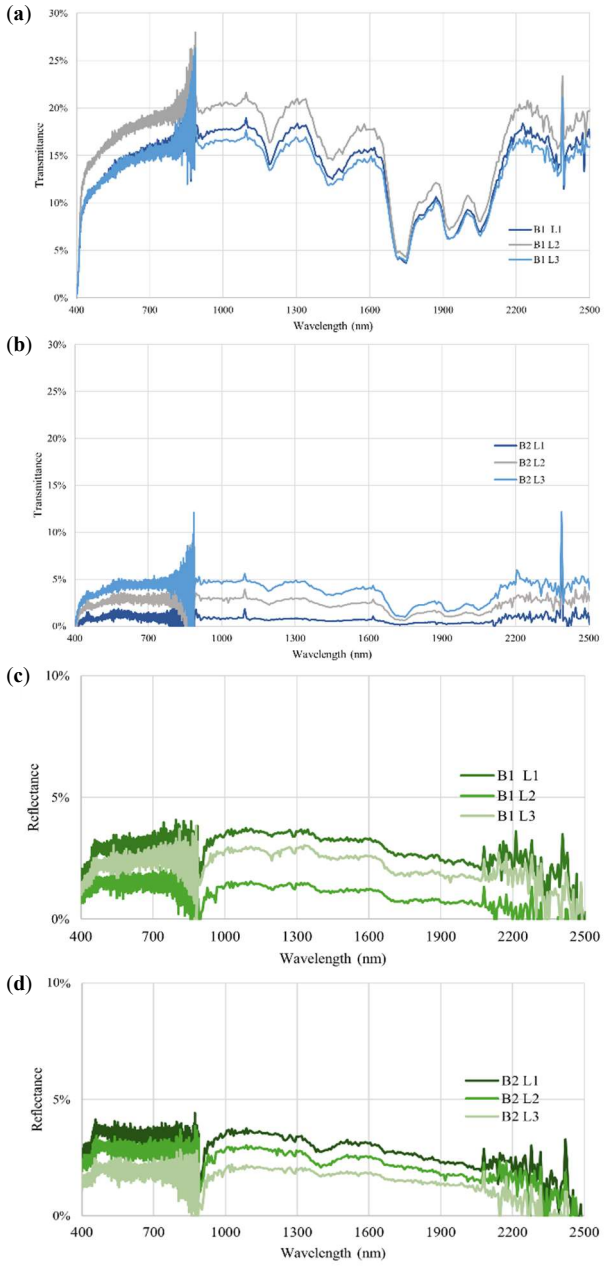

Fig. 6. Characteristic optical behaviour of micro-pods within a braided structure where six braiding parameters have been examined. Each dataset is the average of the results taken from four repeat samples. (**a**) Transmittance, 12-yarns used to construct the braid structure. (**b**) Transmittance, 24-yarns used to construct the braid structure. (**c**) Reflectance, 12-yarns used to construct the braid structure. (**d**) Reflectance, 24-yarns used to construct the braid structure.

The overall transmission levels drastically decreased from 80 % to less than 30 % when comparing the encapsulated samples to braided samples. This is attributed to the coverage provided to the components with the covering yarns in the braided structure absorbing and scattering light. Braiding type B1 showed higher transmittance over type B2, with statistical confirmation ($p < 0.05$) on the significant influence of number of covering yarns towards transmittance across the wavelengths. The lay length of the yarns had no quantifiable effect towards the transmittance behaviour of the braided yarns. There was no major influence on reflectance from the covering yarns. However, lay length was identified to have significant influence on the reflectance behaviour of the braided yarns.

Based on the results of the optical characterisation of the braiding parameters, 12 yarns with a 10 mm lay length were selected to proceed with optimising the transmittance and reflectance behaviour of the braided yarn structure.

C. Pulse Rate Monitoring Textile Glove Validation

E-yarns were produced using the optimal micro-pod and braiding parameters determined above and were integrated into a PR monitoring textile glove prototype. The prototype was validated to assess its functionality and accuracy as a textile based optical sensing system. The prototype of the PR monitoring textile glove is shown in Fig. 7.

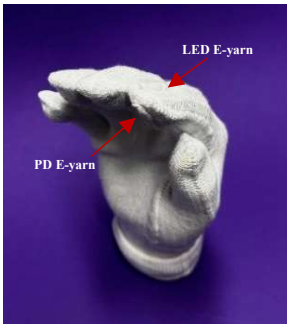

Fig. 7. Photograph of the prototype PR monitoring textile glove. The optical components were incorporated on each side of the index figure.

An example of the raw PPG signals obtained through the prototype glove is shown in Fig. 8.

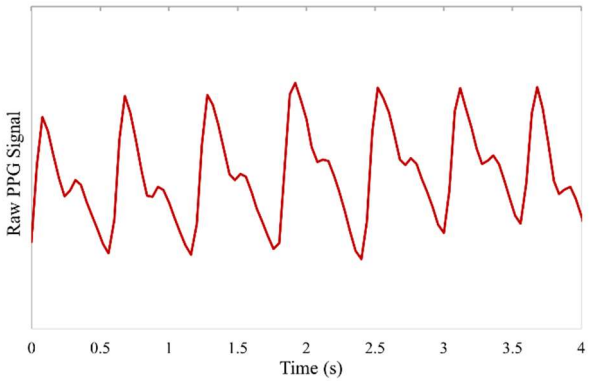

Fig. 8. Example PPG signal recorded using the PR monitoring textile glove.

Experiments were conducted using ten participants, where their pulse rate was recorded. While Heartpy, a heart rate analysis python toolkit designed for PPG data [19], was used to extract the pulse rate of each reading in most cases, there were some limitations in detecting the peaks using this methods as the PPG signal derived through the system was a raw signal without any filtration, artefact removal or

amplification. Further, this signal was exposed to optical and physiological noises such as motion artefacts and ambient light interactions. Hence, some (15 readings) of the pulse rate values were manually calculated from the PPG data gathered when it was believed that the value provided by Heartpy was erroneous.

The final PR outputs of the prototype glove were then compared against the Masimo oximeter PR readings as shown in Fig 9.

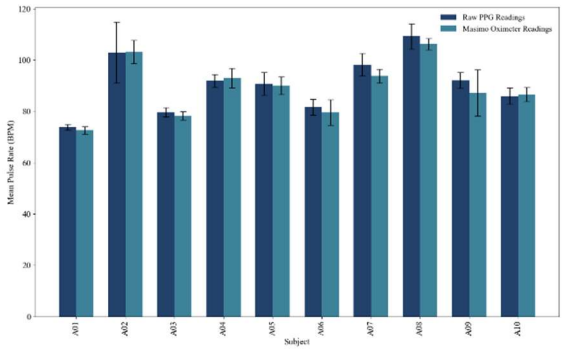

Fig. 9. Chart depicting the PR values collected using the pulse rate monitoring textile glove and commercial PR monitoring system. Each datapoint is the average of five measurements with the error bars depicting the standard deviation.

A comparison of the pulse rate measurements can be seen in Table 6.

TABLE VI. COMPARISON BETWEEN PULSE RATE READINGS FROM THE PR MONITORING TEXTILE GLOVE AND COMMERCIAL PR MONITORING SYSTEM.

Subject	PPG Mean	PPG SD	Masimo Mean	Masimo SD	Percentage Variation
A01	73.80	1.06	72.60	1.52	1.66%
A02	103.00	11.85	103.20	4.49	0.19%
A03	79.64	1.75	78.20	1.64	1.85%
A04	91.89	2.48	93.00	3.74	1.19%
A05	90.73	4.45	90.00	3.46	0.81%
A06	81.64	3.04	79.60	4.98	2.57%
A07	98.19	4.39	93.80	2.68	4.68%
A08	109.24	4.93	106.20	2.17	2.86%
A09	92.14	3.13	87.20	8.98	5.66%
A10	86.00	3.24	86.60	2.70	0.69%

The percentage variation of the PR measured with the PR monitoring textile glove compared to the PR recorded from the commercial system indicated that most of the data gathered using the textile glove was in close agreement showing variations of less than 2 %, with the largest observed discrepancy being 5.66 %.

IV. CONCLUSION

This work successfully presented a pulse rate monitoring textile glove and validated it against a commercial pulse rate monitoring system.

The characterisation of the optical properties of encapsulation was conducted to identify the effect of materials and parameters involved in the encapsulation process of manufacturing optical sensing E-yarns towards the optical behaviour of the E-yarns. Out of the parameters tested, only the resin type was identified to have a significant impact on the transmittance with no significant impact on the reflectance, while the width and thickness of the micro-pod were confirmed to have no significant impact on either transmittance or reflectance behaviours.

Among the three resin types compared, Dymax 9001-EV3.5 resin was identified as the optimal choice due to its high transmittance, moderate reflectance and high consistency, which was validated through statistical analysis.

The optical characterisation of encapsulated micro-pods covered in textile braiding demonstrated that the number of covering yarns significantly impacts transmittance behaviour. A lesser number of covering yarns resulted in higher transmittance. However, this coverage has no influence on the reflectance behaviour. The lay length of braiding was found to significantly affect reflectance, with longer lay lengths resulting in lower reflectance. Nonetheless, lay length had no impact on transmittance. Additionally, it was identified that braiding caused a reduction in light transmission on the encapsulated samples.

The optimised E-yarn design was integrated into a pulse rate monitoring glove capable of effectively measuring PPG signals as a textile based optical sensing system. The PR data extracted through the raw PPG signal recorded with the prototype glove were well aligned with the PR readings recorded with the commercial pulse oximeter.

The extraction, filtering and amplification of the PPG signals extracted from the textile glove using an Arduino-based system is currently in progress to enhance the system's accuracy, reliability and portability. Further, the system's capabilities will be improved to monitor the PRV, oxygen saturation and blood pressure.

ACKNOWLEDGMENT

This work is funded by the Nottingham Trent University, Nottingham, United Kingdom.

The authors would like to thank Kalana Marasinghe for designing the graphical illustration of the E-yarn manufacturing process (Fig.2).

The human trial in this study was conducted in accordance with the approval of the Nottingham Trent University Schools of Art and Design, Arts and Humanities and Architecture, Design and the Built Environment Research Ethics Committee (Application ID 1843617, date of approval 22nd July 2024).

Informed consent was obtained from all the participants involved in the human trial of this study.

Data are contained within the article. The raw datasets collected for the analysis of this study and the anonymised data recorded form the human trial can be found on figshare at 10.6084/m9.figshare.27382098.

REFERENCES

[1] T. Pereira et al., "Photoplethysmography based atrial fibrillation detection: a review," Dec. 01, 2020, Nature Research. doi: 10.1038/s41746-019-0207-9.

[2] M. R. Turchioe, V. Jimenez, S. Isaac, M. Alshalabi, D. Slotwiner, and R. M. Creber, "Review of mobile applications for the detection and management of atrial fibrillation," Heart Rhythm O2, vol. 1, no. 1, pp. 35–43, Apr. 2020, doi: 10.1016/j.hroo.2020.02.005.

[3] S. Lingawi et al., "Cardiorespiratory Sensors and Their Implications for Out-of-Hospital Cardiac Arrest Detection: A Systematic Review," Ann Biomed Eng, vol. 52, no. 5, pp. 1136–1158, May 2024, doi: 10.1007/s10439-024-03442-y.

[4] M. Ghamari, “A review on wearable photoplethysmography sensors and their potential future applications in health care,” Int J Biosens Bioelectron, vol. 4, no. 4, 2018, doi: 10.15406/ijbsbe.2018.04.00125.

[5] C. T. Nguyen, K. T. Nguyen, T. Dinh, V. T. Dau, and D. V. Dao, “Wearable Physical Sensors for Non-invasive Health Monitoring,” in Wearable Biosensing in Medicine and Healthcare, Singapore: Springer Nature Singapore, 2024, pp. 111–132. doi: 10.1007/978-981-99-8122-9_6.

[6] G. A. Roth et al., “Global Burden of Cardiovascular Diseases and Risk Factors, 1990-2019: Update From the GBD 2019 Study,” Dec. 22, 2020, Elsevier Inc. doi: 10.1016/j.jacc.2020.11.010.

[7] H. K. Ballaji et al., “A textile sleeve for monitoring oxygen saturation using multichannel optical fibre photoplethysmography,” Sensors (Switzerland), vol. 20, no. 22, pp. 1–29, Nov. 2020, doi: 10.3390/s20226568.

[8] S. Bagha, S. Hills, P. Bhubaneswar, and L. Shaw, “A Real Time Analysis of PPG Signal for Measurement of SpO2 and Pulse Rate A Real Time Analysis of PPG Signal for Measurement of SpO 2 and Pulse Rate,” 2011. [Online]. Available: https://www.researchgate.net/publication/220043686

[9] E. Gil, M. Orini, R. Bailón, J. M. Vergara, L. Mainardi, and P. Laguna, “Photoplethysmography pulse rate variability as a surrogate measurement of heart rate variability during non-stationary conditions,” Physiol Meas, vol. 31, no. 9, pp. 1271–1290, 2010, doi: 10.1088/0967-3334/31/9/015.

[10] A. A. N. N. and E. S. J. J. P. Madhan Mohan, “Measurement of Arterial Oxygen Saturation (SpO2) using PPG Optical Sensor,” International Conference on Communication and Signal Processing,India, 2016.

[11] Myint CZ, King Hann Lim, Kiing Ing Wong, Alpha Agape Gopalai, and Min Zin Oo, “Blood Pressure Measurement from Photo-plethysmography to Pulse Transit Time,” in IEEE Conference on Biomedical Engineering and Sciences, Malaysia, 2014.

[12] M. Bolanos, H. Nazeran, and E. Haltiwanger, “Comparison of Heart Rate Variability Signal Features Derived from Electrocardiography and Photoplethysmography in Healthy Individuals,” in 28Th IEEE EMBS Annual International Conference, 2006.

[13] A. Schäfer and J. Vagedes, “How accurate is pulse rate variability as an estimate of heart rate variability?: A review on studies comparing photoplethysmographic technology with an electrocardiogram,” Jun. 05, 2013. doi: 10.1016/j.ijcard.2012.03.119.

[14] M. Rothmaier et al., “Photonic textiles for pulse oximetry,” Springer, 2005. [Online]. Available: http://www.brochiertechnologies.com

[15] G.-S. Ryu et al., “Flexible and Printed PPG Sensors for Estimation of Drowsiness,” IEEE Trans Electron Devices, vol. 65, no. 7, pp. 2997–3004, Jul. 2018, doi: 10.1109/TED.2018.2833477.

[16] D. Han et al., “Pulse Oximetry Using Organic Optoelectronics under Ambient Light,” Adv Mater Technol, vol. 5, no. 5, May 2020, doi: 10.1002/admt.201901122.

[17] H. Xu, J. Liu, J. Zhang, G. Zhou, N. Luo, and N. Zhao, “Flexible Organic/Inorganic Hybrid Near-Infrared Photoplethysmogram Sensor for Cardiovascular Monitoring,” Advanced Materials, vol. 29, no. 31, Aug. 2017, doi: 10.1002/adma.201700975.

[18] A. Satharasinghe, T. Hughes-Riley, and T. Dias, “Photodiode and LED embedded Textiles for wearable healthcare applications,” 19th World Textile Conference (AUTEX), pp. 11–15, 2019.

[19] P. Van Gent, H. Farah, N. Van Nes, and B. Van Arem, “Analysing Noisy Driver Physiology Real-Time Using Off-the-Shelf Sensors: Heart Rate Analysis Software from the Taking the Fast Lane Project,” J Open Res Softw, vol. 7, no. 1, p. 32, Oct. 2019, doi: 10.5334/jors.241.